College of Saint Benedict and Saint John's University

# DigitalCommons@CSB/SJU

2016

# Pulse and Orbital Periods of ASAS182612

Ariel F. Lusty
*College of Saint Benedict/Saint John's University*, aflusty@csbsju.edu

Follow this and additional works at: https://digitalcommons.csbsju.edu/honors_thesis

Part of the Physics Commons

PULSE AND ORBITAL PERIODS OF ASAS182612

UNDERGRADUATE THESIS
College of Saint Benedict/Saint John's University
In Partial Fulfillment
Of the Requirements for Distinction
In the Department of Physics
by Ariel F. Lusty
May 2016

Title: Pulse and Orbital Periods of ASAS182612

By Ariel Lusty

Approved by:

_____

Thomas Kirkman

Advisor, Associate Professor of Physics

_____

Adam Whitten

Associate Professor of Physics

_____

Sarah Yost

Associate Professor of Physics

_____

Jim Crumley

Chair, Professor of Physics

_____

Emily Esch

Director, All College Thesis Program

ABSTRACT

Physicists S.V. Antipin, K.V. Sokolovsky, and T.I. Ignatieva began
observations of the variable star ASAS182612 in 2005, and found it to be the first
known eclipsing binary with a type II Cepheid component in our galaxy. A month
after Antipin's publication, the American Association of Variable Star Observers
(AAVSO) sent out an alert to campaign for observations of ASAS182612. From July
2007 to November 2015, 147 nights of multi-filter photometric data have been
collected for ASAS182162. The pulsation period found was $4.1591 \pm 0.0001$ days and
the orbital period $51.352 \pm 0.016$ days.

1. INTRODUCTION

Variable stars are stars that change brightness, and need to be systematically observed over decades to determine their long-term behavior. Around 1780, astronomer Edward Pigott and John Goodricke divided variables according to the nature of their light curve into novae, long-period variables, and short-period variables. A century later, Edward Pickering devised a classification system for variable stars that ranges from Types I (novae) to V (Algol type eclipsing variables). While the shape of a star's light curves allows classification, what is of primary interest is the physical nature of the variability.

Pigott and Goodricke speculated that eclipses were causing the variability of some stars. In 1880, Henrietta Swan Leavitt supported the eclipsing hypothesis by carefully observing a star's light curve. In 1889, Herman Vogel used spectroscopy and the Doppler effect to directly observe the orbital motion and demonstrate the eclipsing effects. During an eclipse, the star dims and yields an increase in the apparent magnitude. Around 1915, Arthur Eddington established the pulsational nature of Cepheids, cluster type variables, and the long-period variables. After 1950, the cause of pulsation was established as the thermodynamic effect of hydrogen and helium in the outer layer of the stars (Percy 2007). The relationship between a Cepheid variable's pulse and luminosity has been used to determine distances to far-away galaxies (Saladyga 2013).

In 1997, Bohdan Paczyński suggested using small, automated instruments for bright star surveys (Pojmański 2002). In 2000, Grzegorz Pojmański catalogued

3900 variable stars in the equatorial zone of the Northern Hemisphere and titled

this catalogue the All Sky Automated Survey (ASAS). Today, ASAS is dedicated to

constant photometric monitoring of the whole available sky, approximately $10^7$ stars

brighter than magnitude 14. The project's ultimate goal is detection and

investigation of any kind of photometric variability, and thus to contribute to our

understanding of the universe (Pojmański 2015).

The data catalogued by 2004 was minimal for the variable ASAS182612, so

S.V. Antipin, K.V. Sokolovsky, and T.I. Ignatieva observed the star in 2005 with the

50-cm Maksutov telescope of the Crimean Laboratory to further explain its light

variations, and found it to be the first known eclipsing binary with a type II

Cepheid component in our galaxy (Antipin, Sokolovsky, and Ignatieva 2007). A

month after Antipin's publication, the American Association of Variable Star

Observers (AAVSO) sent out an alert to campaign for observations of ASAS182612.

The Saint John's University Observatory Clear Sky Chart was used to

predict the cloud cover each evening. Observations were only taken for evenings

where there are no clouds, as seen from the Saint John's Observatory. The

observation dates range from 2454301.67 (July 20, 2007) to 2457342.51 (November

16, 2016).

*We have collected 147 nights of multi-filter photometric data for ASAS182612*

*since 2007 and compared it to the data published by the AAVSO.*

## 2. THEORY

### Magnitude

The apparent magnitude is the standard unit for measuring the brightness of a star

or other celestial object. Stars magnitudes are defined by the relationship:

$$m_1 - m_2 = -2.5 \log\left(\frac{B_1}{B_2}\right) \tag{1}$$

where $m_1$ and $m_2$ are the magnitudes of two stars and $B_1$ and $B_2$ are their physical

brightnesses (Percy 2007). Greek astronomer Hipparchus (190-120 BCE) formulated

the first magnitude system, where magnitudes ranged from 1 to 6, with 1

corresponding with the brightest magnitude. More recently, brightness is measured

relative to the standard reference star, Vega, which is used for its black body and

non-variable characteristics. Celestial objects brighter than Vega have negative

magnitudes. Brightness depends on flux, and decreases with distance from Earth.

Flux is also reduced by the absorption in Earth's atmosphere, but magnitudes are

adjusted to correct for this effect by using in-frame standards.


### Color Index

Star colors are measured with a photometer, with filters that transmit different

color bands in the spectrum (see Camera section). Star magnitudes are measured

through each filter, and the differences in magnitude, or color indices, demonstrate

the relative amounts of two colors. $B$-$V$ is a common color index:

$$B - V = 2.5 \log\left(\frac{F_V}{F_B}\right) + constant \tag{2}$$

where $F_V$ is the flux through the visible (V) filter, and $F_B$ is the flux through the blue (B) filter. In the absence of interstellar absorption the flux ratio $\frac{F_V}{F_B}$ should be independent of distance and hence an intrinsic property of the star related to its temperature. However, dust grains in the interstellar medium absorb wavelengths of blue light, which makes stars appear redder than they really are (Swinburne 2016).

4. OBSERVING

Camera

A charged-coupled device (CCD) within a Santa Barbara Instrument Group (SBIG) STL-1001E camera was used to count photons transmitted through the Meade 12" LX200 Schmidt-Cassegrain Catadioptric telescope (see Figure 1). Photons are collected and counted on an array of approximately 1000x1000 microscopic light-sensitive pixels. The light on each pixel is recorded as an integer; the resulting 1000x1000 matrix is an image that can be used during data processing (see Results). When photons hit a pixel, electrons are released by the photoelectric effect and stored in place during the exposure. The pixels are defined by an array of gates formed on the CCD chip. The CCD transfers charge in a pixel by manipulating the voltage on the gates so the pixel's electrons move down vertical rows from one pixel to the next. Finally, a pixel's charge is placed in a capacitor and the resulting voltage, which is proportional to the charge, is measured with an Analog-to-Digital Converter (ADC). The digital data—$10^6$ integers—is saved as a FIT file using the program, CCDOps.
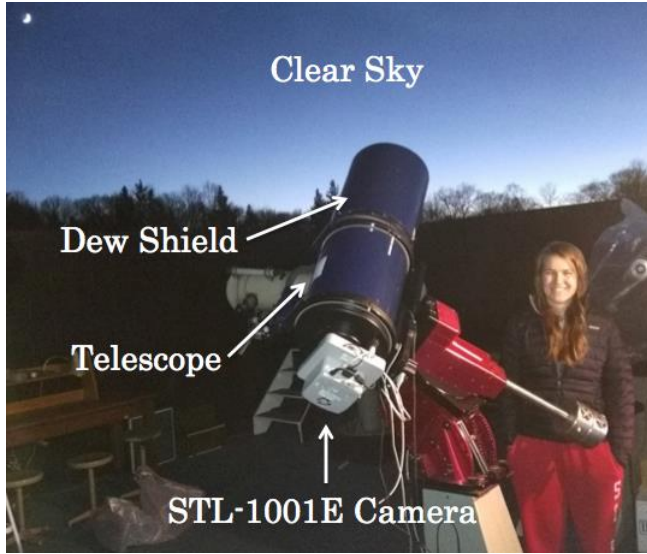
Figure 1: Photograph of Telescope and Camera Setup.

Inside the camera, an SBIG FW8-STL filter wheel (see Figure 2) allows for switching between B (blue), V (visible or green), R (red), and I (infrared) filters. Each filter allows transmission for a range of wavelengths, centered on a particular wavelength.



Figure 2: SBIG filter wheel with B, V, I, R, and blank filters; the additional filters (not used) are sloan g', r', i' filters.

The camera uses thermoelectric (TE) cooling, where a current passes through two dissimilar conductors in a circuit and causes a temperature difference between them, to cool the camera to -20 degrees Celsius. The camera is cooled prior to each collection run to reduce random readout noise generated by thermal electrons and allow for longer exposures (SBIG 2003a). It is uncertain as to why, but water blobs appear on the image when the CCD is first powered. It is possible that water condenses on the CCD due to the decrease in temperature. On startup, images are repeatedly taken until the blob is entirely 'evaporated.' Once the blobs have been cleared, flat frames are collected.

Frames

Flat fields and dark frames, or "flats" and "darks," are essential in calibrating and improving the overall quality of the images taken by the camera. Flats, or evenly illuminated images, were taken after the blobs were cleared. Three flats were taken for each filter in three different locations in the sky at twilight. The twilight sky provides a blank, evenly lit source for flat fields. Flat field collection sites were starless, dark spots in the sky, as displayed by TheSkyX program. The best location in the sky is in an area just east of the zenith, or the point in the sky directly above the observatory, as this area of the sky exhibits the least brightness gradient. Sites where TheSkyX showed no stars in the sky were chosen to prevent stars from appearing in the images. At the start of flat field collections, flats were taken using

the minimum exposure time, 0.12 seconds. Increments of around 0.10 seconds were added to the 0.12 seconds, and flats continued to be taken until 1-second exposures were reached. It was around the 1-second exposure time where stars began to appear. The primary purpose of using flat fields is to eliminate a vignetting effect, but they also correct for dust particles on the lens (Starizona 2014). The recommended flat field value, or number of electrons the photons created, for the STL-1001E camera was 30,000 – 57,000 Analog Digital Units (ADUs), which could be verified using the histogram feature in CCD Ops. Flats are divided into the uncalibrated images taken later to remove aberrations. Darks, or evenly dark images, are taken with the shutter closed. Darks are used to subtract the consistent flux of electrons that happens even in the absence of light. Several factors cause noise, including dark current, temperature, and camera characteristics. Dark current is the residual electric current flowing in the CCD when there is no illumination. This combined with varying camera characteristics can produce counts (that seemingly illuminate) certain pixels. Sets of images at 300, 120, 60, 30 and 15 seconds were taken individually and later combined with the uncalibrated images.

TheSkyX

TheSkyX program connects the computer to the telescope, and allows the user to move the telescope to examine different locations in the sky. TheSkyX provides information on stars and planets, including their names and magnitudes.

Focus

To begin the focusing process each evening, a dim star of magnitude 4 or 5 is

selected in TheSkyX. The telescope is aimed at that star, and then CCDOps is

opened to Focus mode. The focuser concentrates the star target in a few pixels,

which reduces the relative amount of noise in an image. Each pixel has its own

amount of noise. The focuser is manually adjusted to maximize pixel counts so the

star's light is concentrated in the smallest number of pixels, and the noise is thus

reduced.

CCDOps

The CCDOps program was used to connect to the camera/CCD. Some of the

program's features include allowing the user to set the camera's temperature, focus,

and filter. Its most important purpose, however, is to collect black and white images

that are analyzed to find stars' pulse and orbital periods (SBIG 2003b). It is in

CCDOps where we began to process our data, as it was used to dark subtract and

flat field images of IC 4665 and KU Her (see Results).

IC 4665

IC 4665 (Figure 3) is a cluster of stars used to calibrate images. IC 4665 was used

because it is within telescope range (Dec: -5° < δ), a size that matches our camera

(~15'), has little reddening, and contains calibrated sources (Kirkman 2015). Three

sets of frames were collected for each filter at different durations: 15 seconds for the

B filter, 15 or 7.5 seconds for the V filter, 3 seconds for the R filter, and 2 seconds for the I filter. These particular durations were determined in previous years to typically produce optimal ADC values of less than 50,000 ADU.
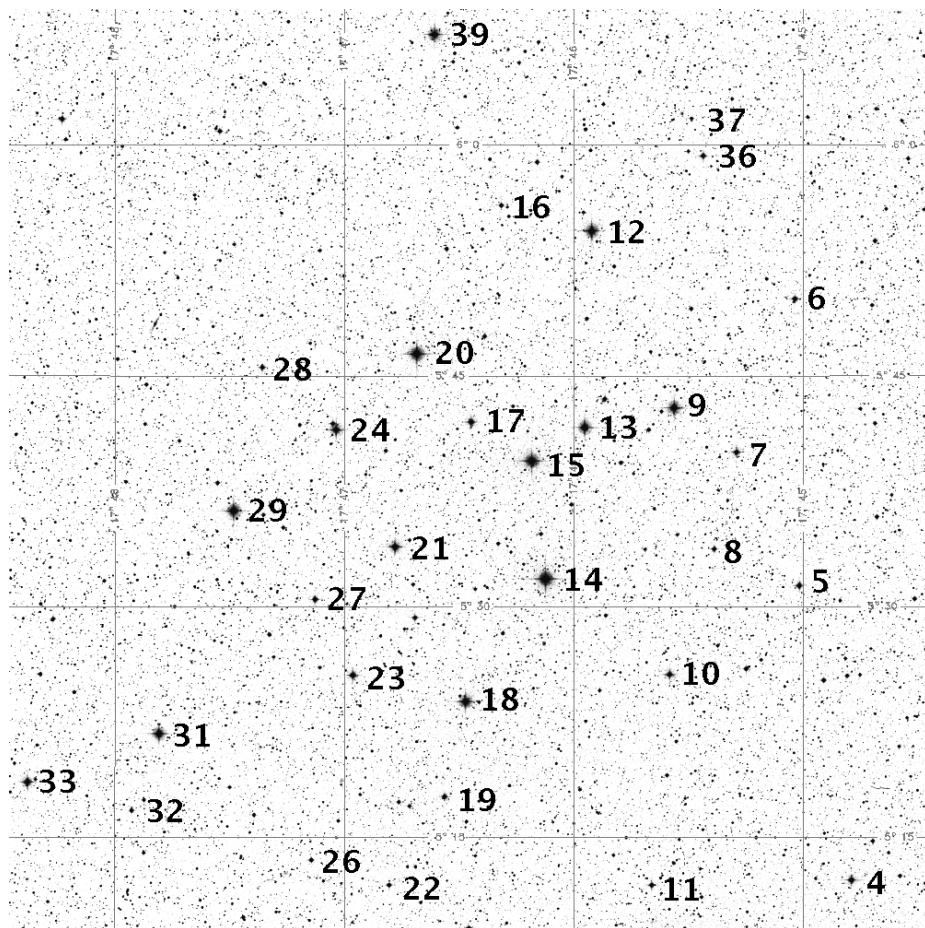


Figure 3: Digitized Sky Survey image of the open cluster IC 4665. Stars 24, 29, 21, 27, 23, 31, 32 and 33 were used for calibration.

KU Her

ASAS182612 is located near the star KU Her. Three sets of frames for the KU Her area were collected after those for IC 4665, but at different intervals for each filter: 120 seconds for B, 60 seconds for V, 30 or 15 seconds for R, and 15 or 5 seconds for I.
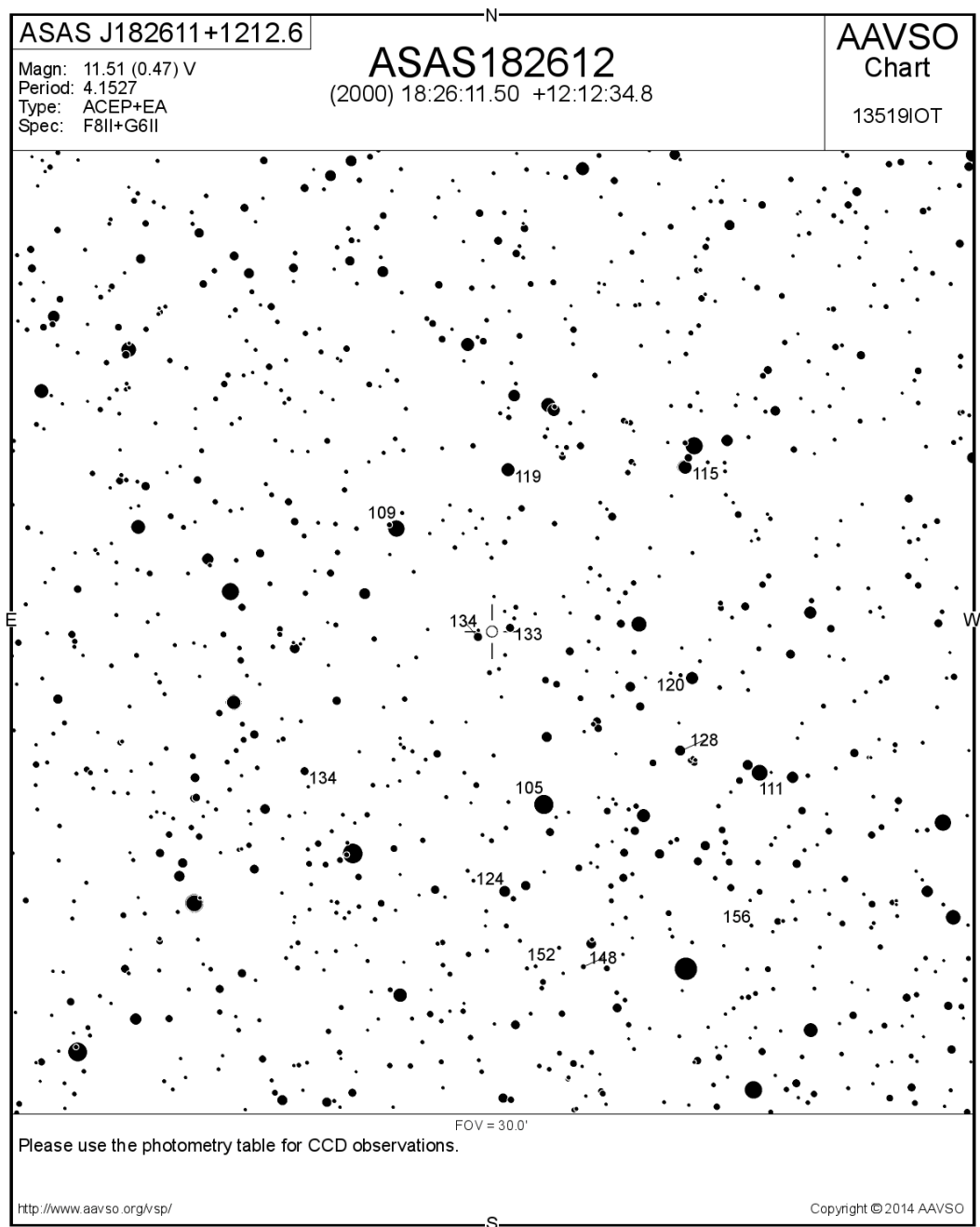
Figure 4: AAVSO Chart of ASAS182612, which is illustrated as the white circle.

## 5. CLEANING DATA

### AAVSO

The AAVSO collects and archives observations into an online database. All of the data for ASAS182612 collected by other observers since 2007 were downloaded from the AAVSO database. The data downloaded from AAVSO contains fields including the Julian dates, magnitudes, filters, and observer names. The data was split by filter type and saved in comma separated value (.csv) files. The data contained duplicates, or multiple observations of the same star separated by minutes. We believe errors are largely systematic, so averaging does little to reduce the error, which would give undue weight to multiple repeated measurements. Each filter file was run through a Fortran program to average the magnitudes and Julian dates for observations made by the same observer on the same Julian day.

### Chauvenet's Criterion

Once the duplicates were removed, Chauvenet's criterion was used in Mathematica to find points that deviated substantially from others. Chauvenet's criterion rejects points that, given the number of samples, deviate an unlikely amount from the mean (i.e. the probability of finding such a large deviation was less than $\frac{1}{2N}$). The criterion was repeated until all outliers were removed. "Clean" files, or those that had duplicates and outliers removed, were exported and ready to be fit to a nonlinear function and plotted. Chauvenet's criterion was used for both AAVSO and CSB/SJU data.

6. PLOTTING DATA

Nonlinear Plots

The nonlinear model is a more accurate depiction of brightness variations than the linear model because it takes into account the acceleration of the star's pulsation. However, nonlinear fits require starting guesses for parameters. We found these by using a linear model. The linear model used the following truncated Fourier series to represent the measured magnitude:

$$f[x] = g1\ Sin[a\ x] + g2\ Cos[a\ x] + g3\ Sin[2a\ x] + g4\ Cos[2\ a\ x] + g5\ Sin[3\ a\ x] +$$

$$g6\ Cos[3\ a\ x] + g7\ Sin[b\ x] + g8\ Cos[b\ x] \tag{3}$$

where $a = \frac{2\pi}{4.15801}$ and $b = \frac{4\pi}{51.3333}$, which are the values for the pulse and orbital frequencies from previous years' results, respectively. The orbital angular frequency has $4\pi$ in the numerator because a tidally elongated star shows minimum area twice per orbit: once when the star is front of the binary companion, and once when the star is behind the binary companion. The nonlinear model was found using the best fit parameters from the linear model fit, g1 through g8, and the following function:

$$f[x] = k1 + k2\ Sin[(a\ x + c\ x^2/2)] + k3\ Cos[(a\ x + c\ x^2/2)] + k4\ Sin[2(a\ x + c\ x^2/2)] +$$

$$k5\ Cos[2(a\ x + c\ x^2/2)] + k6\ Sin[3(a\ x + c\ x^2/2)] + k7\ Cos[3(a\ x + c\ x^2/2)] +$$

$$K1\ Sin[b\ x] + K2\ Cos[b\ x] \tag{4}$$

The Nonlinear Model Fit function in Mathematica was used to find the best fit parameters and the confidence intervals of k1, k2, k3, k4, k5, k6, k7, a, b, and c, which are used to plot the pulse periods. Just as for the linear model, a and b are

respectively the pulse and orbital frequencies. The value c is the acceleration. The

values of K1, K2, a, b, and c were found from equation 4, and were used to fit the

data to the orbital period function. The pulse period can be fit to function 5, and the

orbital period can be fit to function 6:

$$fp[x] = k1 + k2\,Sin[(a\,x + c\,x^2/2)] + k3\,Cos[(a\,x + c\,x^2/2)] + k4\,Sin[2(a\,x + c\,x^2/2)] +$$

$$k5\,Cos[2(a\,x + c\,x^2/2)] + k6\,Sin[3(a\,x + c\,x^2/2)] + k7\,Cos[3(a\,x + c\,x^2/2)] \qquad (5)$$

$$fo[x] = K1\,Sin[b\,x] + K2\,Cos[b\,x] \qquad (6)$$

Plotting Pulse Period

In order to clearly display the results at one frequency, we must subtract the results

at the other frequency. This is called "pre-whitening." The times from the "Clean"

data, which is still separated by filter, is input as x into equation 6. These new

values are then subtracted from their "Clean" magnitudes to produce magnitudes

that are plotted in figure 5 for the AAVSO data, and figure 6 for the CSB/SJU data.

We plot equation 5 for comparison. The modulus of the times $Mod[a\,t + \frac{1}{2}\,c\,t^2, 2\pi]$ is

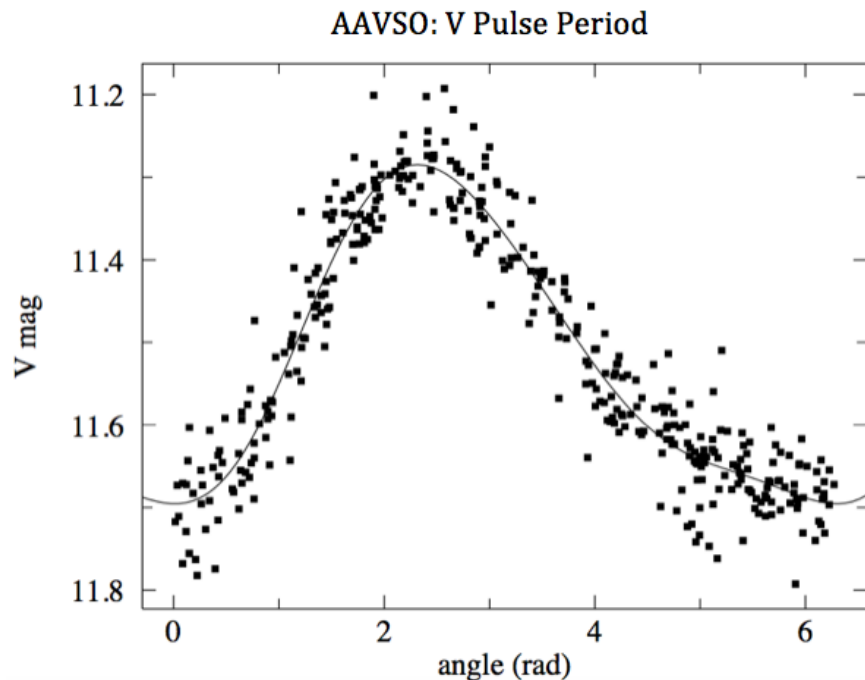taken to find the angle in radians of the pulse period.

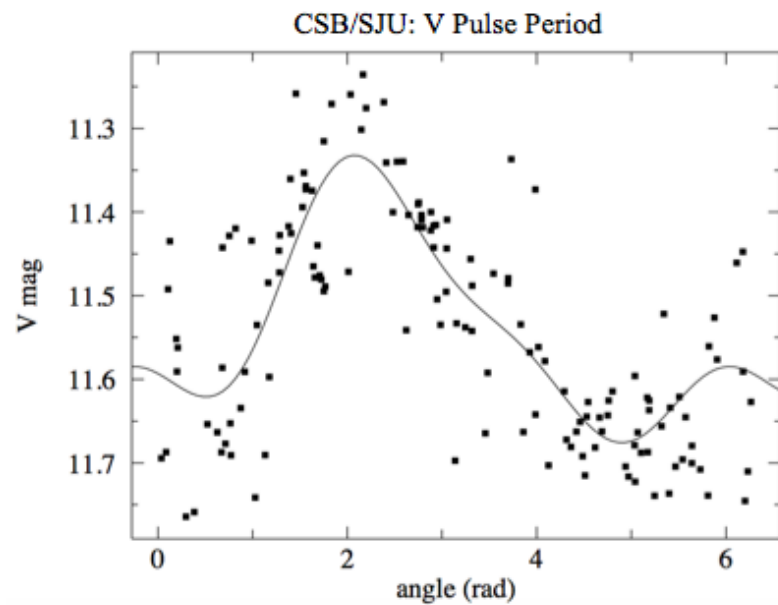Figure 5: The AAVSO V data with orbital effects subtracted.



Figure 6: The CSB/SJU V data with orbital effects subtracted. Note some data points are ~0.2 magnitudes away from the function curve.

Plotting Orbital Period

The times from the "Clean" data is input as x into equation 5. These new values are then subtracted from their "Clean" magnitudes to produce magnitudes that are plotted in figure 7 for the AAVSO data, and figure 8 for the CSB/SJU data. The modulus of the times, $Mod[t, \frac{4\pi}{b}]$ , is done.
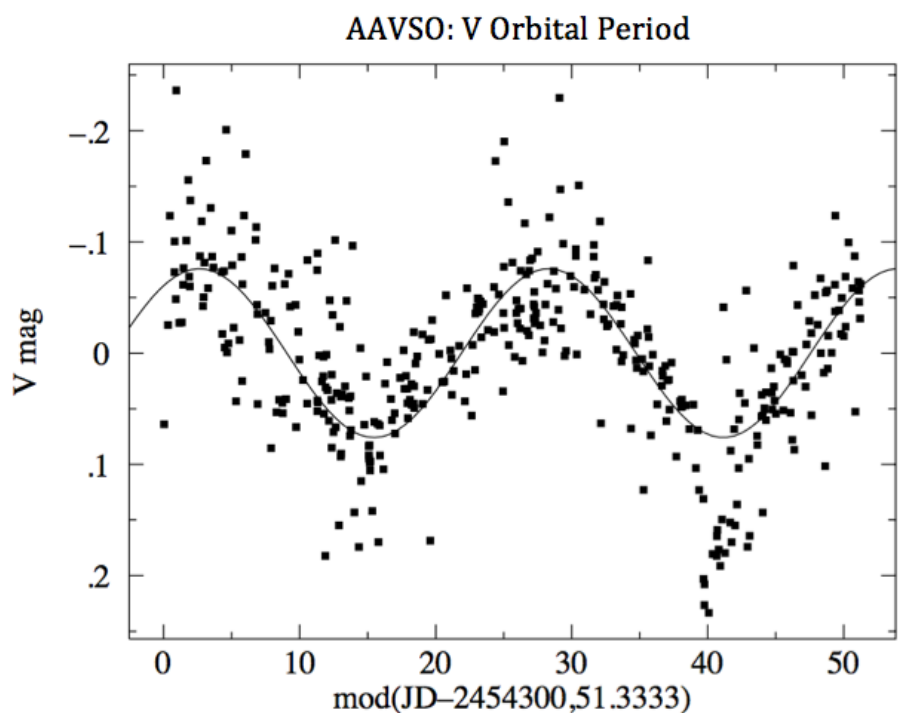


Figure 7: The AAVSO V data with pulse effects subtracted. Note the magnitudes are unusually dim at ~15 and ~40 days. We suspect that the star was eclipsed by or eclipsed its binary companion at these times.
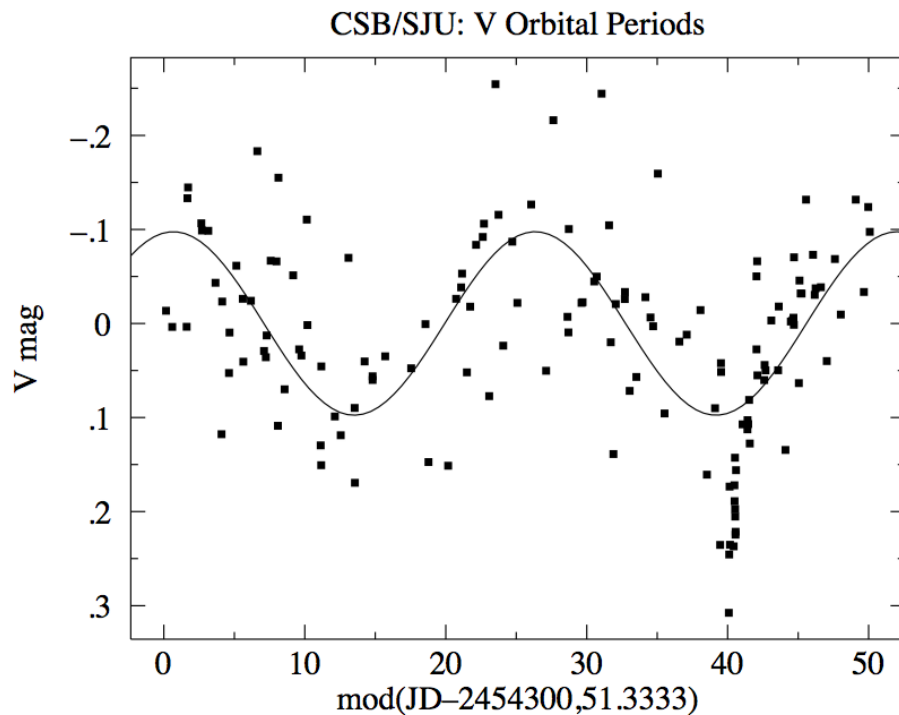
Figure 8: CSB/SJU V data with pulse effects subtracted. Note the magnitudes are unusually dim at ~40 days.

Comparisons of Pulse and Orbital Periods

The pulse period and its error for "All" filters for the AAVSO data are found by taking the weighted averages of the pulse periods for the B, V, R, and I filters. The pulse period and its error for "All" filters for the CSB/SJU data is found by taking the weighted average of the V, B-V, R-I and I filters (Figure 9).
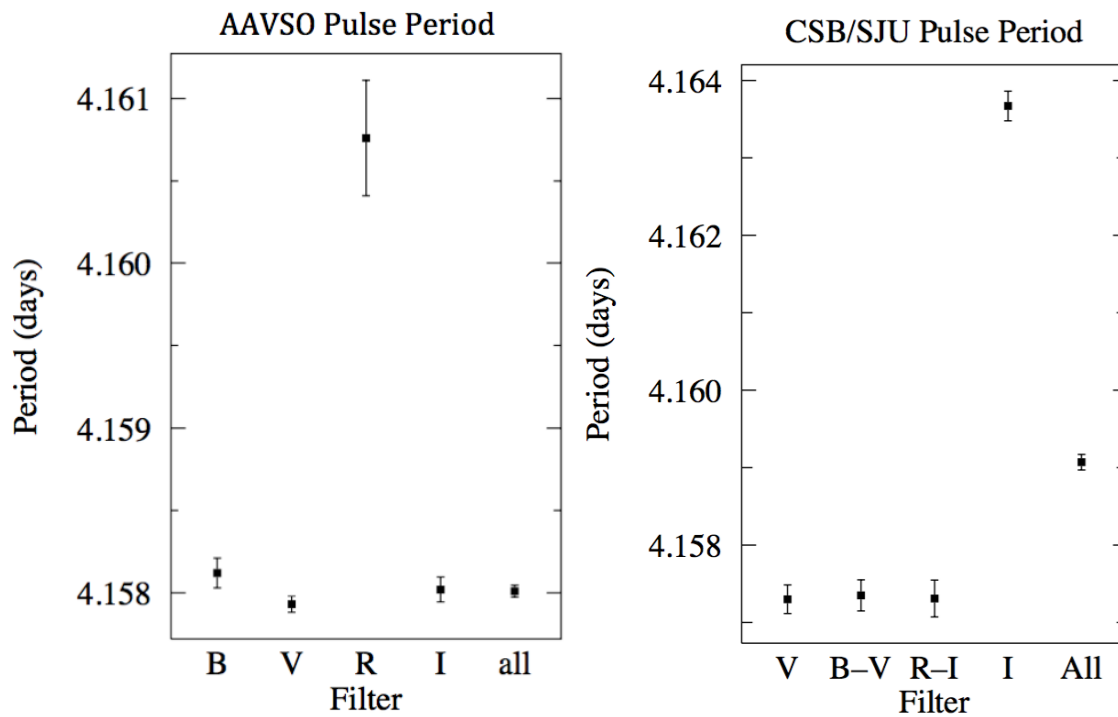
Figure 9: Comparison of AAVSO and CSB/SJU pulse periods. The margin of error is larger for the pulse period found using the R filter for AAVSO because there were fewer data points.

The orbital period and its error for "All" filters for both datasets are found in the same way as the pulse period (Figure 10).
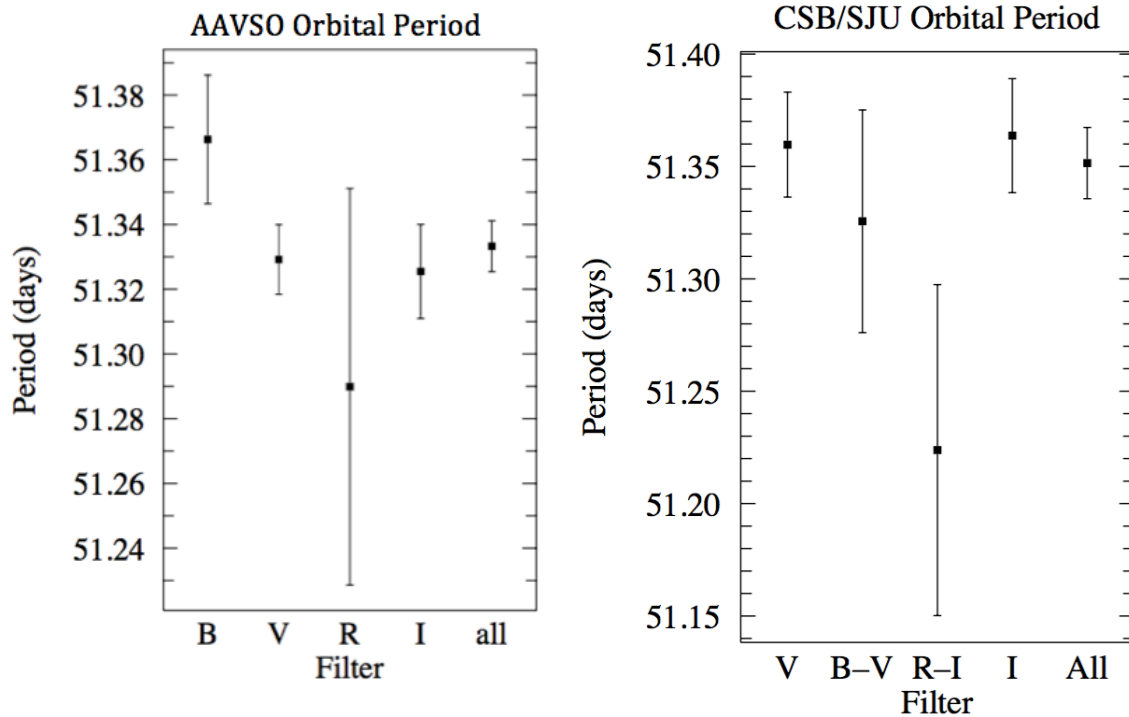
Figure 10: Comparison of AAVSO and CSB/SJU orbital periods. The orbital periods found using the R filter are slightly lower than the other filters, but they are fairly consistent between the AAVSO and CSB/SJU data.

Acceleration

Similarly to finding the pulse and orbital periods, the acceleration and its error for "All" filters for the AAVSO data are found by taking the weighted averages of the B, V, R, and I filters. The acceleration and its error for "All" filters for the CSB/SJU data is found by taking the weighted average of the V, B-V, R-I and I filters (Figure 11).
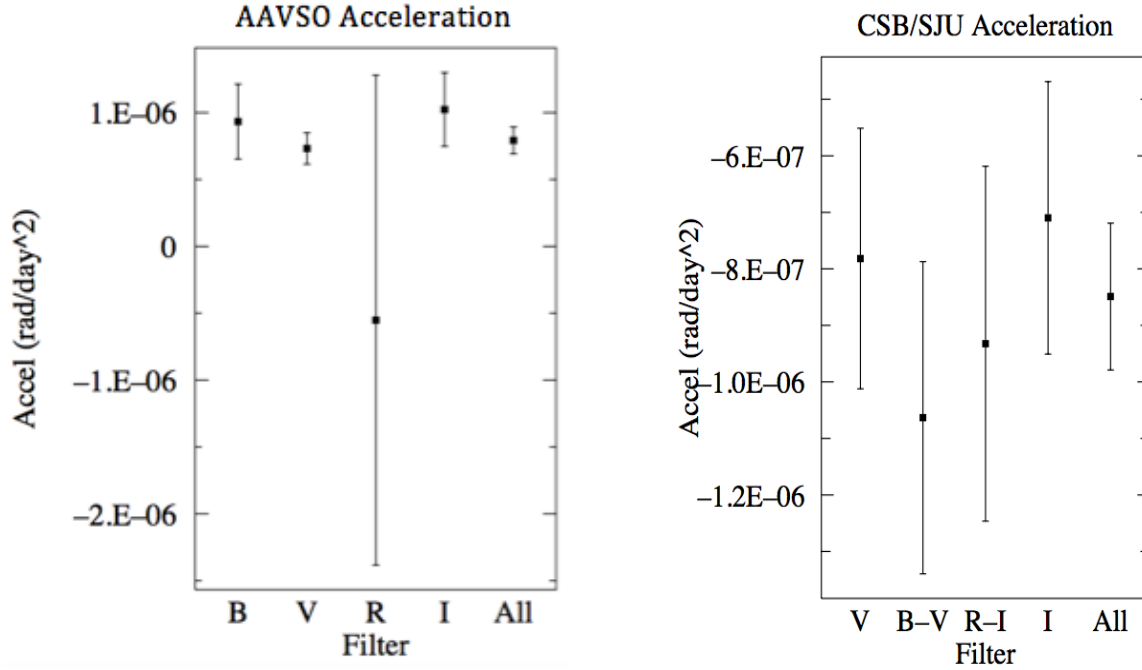
Figure 11: Comparison of AAVSO and CSB/SJU accelerations. The margins of error are higher for CSB/SJU data since there are fewer data points.

| | AAVSO | CSB/SJU |
|---|---|---|
| Pulse Period (days) | 4.15801 ± 0.00004 | 4.1591 ± 0.0001 |
| Orbital Period (days) | 51.3333 ± 0.0079 | 51.352 ± 0.016 |
| Acceleration (rad/day^2) | 7.9E-7 ± 1.0E-7 | -8.5E-7 ± 1.3E-7 |

Figure 12: Final results. Although not within margins of error of each other, the results of pulse period and orbital period between the two datasets were close. According to the AAVSO dataset, the star's pulsation seems to be accelerating, but the CSB/SJU dataset shows deceleration.

GAIA

The Graphical Astronomy and Image Analysis Tool (GAIA) displays the images captured after flat fielding and dark subtracting. The annotation toolbar was used to add labels to reference stars and to ASAS182612.
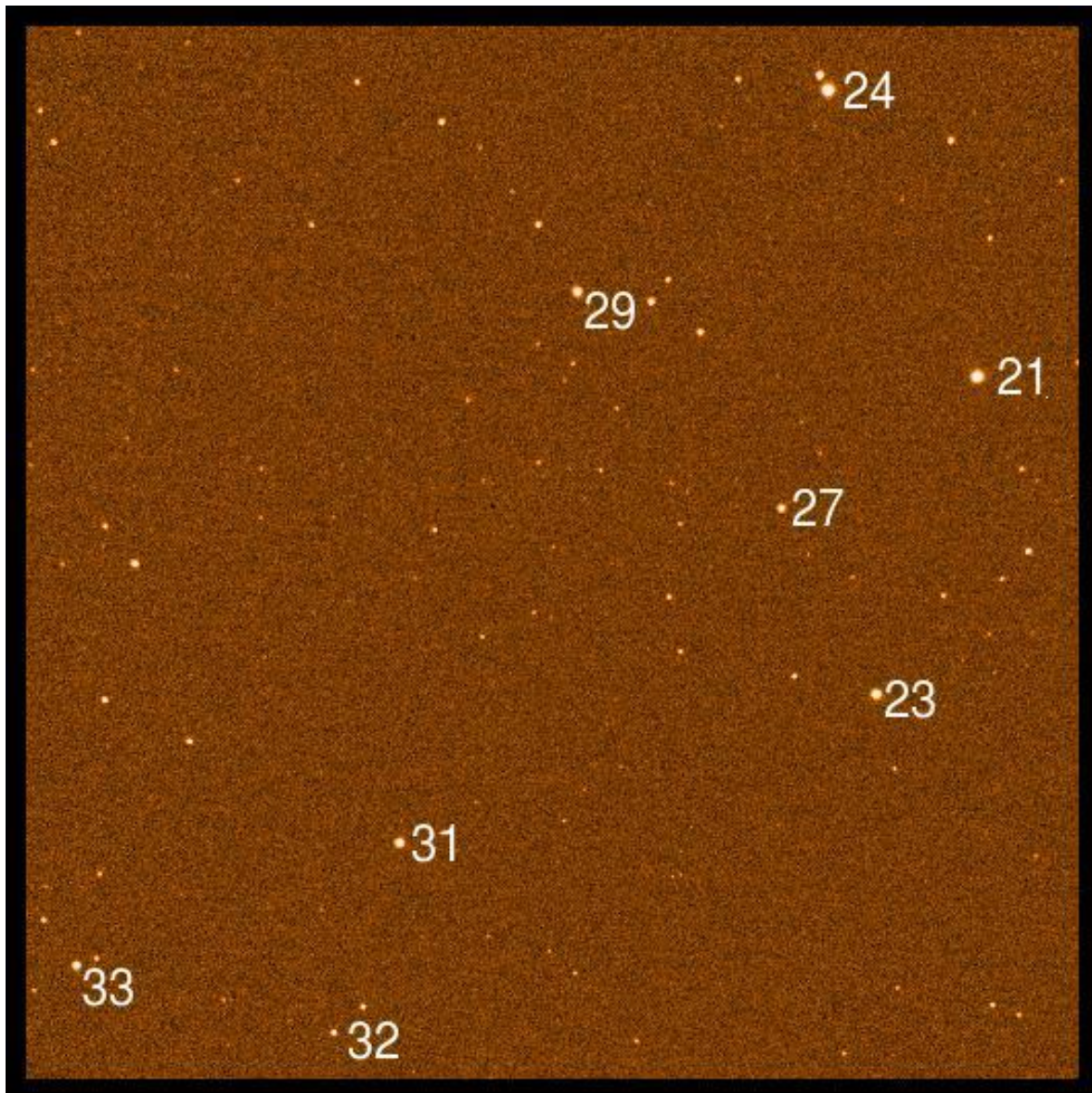


Figure 13: GAIA histogram equalized image of the open cluster IC 4665 captured on September 21, 2015 using I filter.
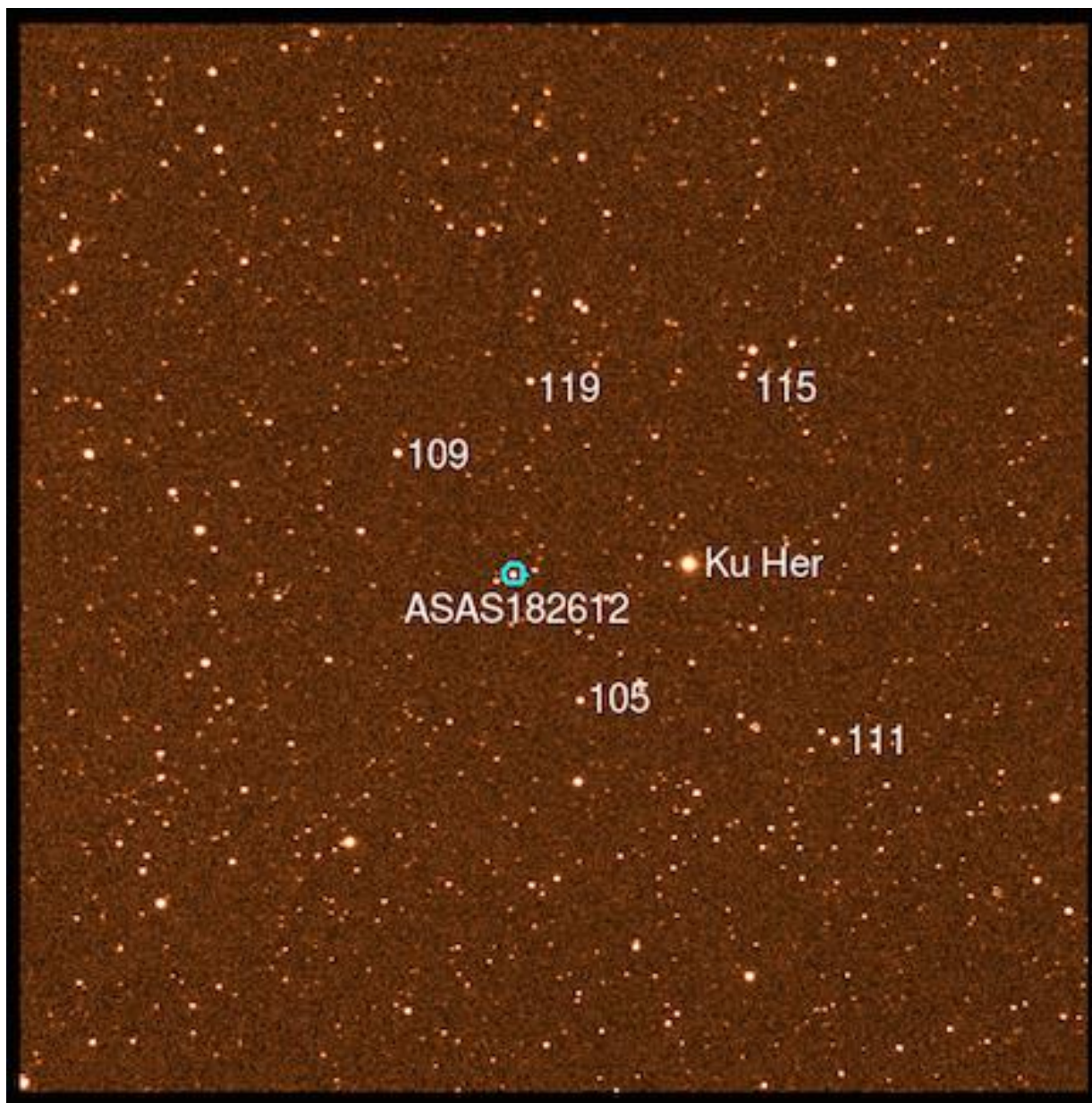
Figure 14: GAIA histogram equalized image of KU Her captured on September 21, 2015 using I filter.

6. CONCLUSIONS

The ~0.2 magnitude gap between the function curve and the data points in Figure 6 indicates that there may be an error in the CSB/SJU data. The source for the error is unknown. The increased magnitudes at ~15 days and ~40 days (Figure 7) indicate an eclipse, or where the binary companion is passing in front or behind ASAS182612. There does not appear to be an increased magnitude at ~15 days in Figure 8, which indicates either there is an error in the CSB/SJU data or that there is an insufficient amount of data to support that there is an eclipse occurring at that time.

Last year, Joseph Hoppert concluded that ASAS182612 was accelerating. However, because of the negative accelerations found in the CSB/SJU data analysis, which conflict with the positive accelerations found in the AAVSO data analysis, it cannot be concluded whether the star is accelerating or not (Figure 11). Hoppert had combined both datasets, whereas they are examined separately here, which could be the reason for the disparate conclusions.

The CSB/SJU orbital period was found to be 0.04% higher than the AAVSO orbital period, and the CSB/SJU pulse period was found to be 0.03% higher than the AAVSO pulse period (Figure 12). One reason for the variations between the AAVSO and CSB/SJU results is from using color indices, B-V and R-I, to find seemingly more accurate results. Unrelated to the use of color indices, the angular acceleration of the pulsation period for the AAVSO data was positive, while the acceleration for the CSB/SJU data negative.  The accuracy of the CSB/SJU results, however, may be

doubted due to the great divergence of accelerations from those from AAVSO. Thus, we can neither prove nor refute that the pulse of the variable star ASAS182162 is accelerating.

## 7. ACKNOWLEDGEMENTS

## 8. BIBLIOGRAPHY

Antipin, S.V., K.V. Sokolovsky, and T.I. Ignatieva. 2007. "TYC 1031 01262 1: The First Known Galactic Binary with a Type II Cepheid Component." *MNRAS* 379 (L60–L62). http://arxiv.org/pdf/0705.0605v2.pdf.

Cargile, P.A., and D.J. James. 2010. "Employing a New, BVIc Photometric Survey of IC 4665 to Investigate the Age of This Young Open Cluster." *The Astronomical Journal*, no. 140: 677–91.

Feast, Michael, and Patricia Whitelock. 1997. "Galactic Kinematics of Cepheids from Hipparcos Proper Motions." *Royal Astronomical Society*, 683–93.

Hoppert, Joseph E. 2015. "Photometric Extraction of the Pulse and Orbital Periods of ASAS182612: Eclipsing Binary with a Type II Cepheid Component." *St. John's University*.

Kirkman, Thomas. 2015. "Photometry Lab Manual." *St. John's University*.

Lodieu, N., and G. Carraro. 2009. "The Mass Function of IC 4665 Revisited by the UKIDSS Galactic Clusters Survey." *Astronomy & Astrophysics*. http://www.iac.es/galeria/nlodieu/media/articles/paper_IC4665_GCS_opt.pdf.

Percy, John R. 2007. *Understanding Variable Stars*. Cambridge University Press.

Pojmański, Grzegorz. 2002. "The All Sky Automated Survey. Catalog of Variable Stars." *ACTA ASTRONOMICA* 52: 397–427.

———. 2015. "The All Sky Automated Survey." *The All Sky Automated Survey*. http://www.astrouw.edu.pl/asas/?page=main.

Rowe, Jason, and Sawyer Hogg. 2001. "Variable Stars in Galactic Globular Clusters." *The Astronomical Journal*. http://iopscience.iop.org/article/10.1086/323719/pdf.

Saladyga, M. 2013. "Variables: What Are They and Why Observe Them?" *American Association of Variable Star Observers*. https://www.aavso.org/variables-what-are-they-and-why-observe-them.

SBIG. 2003a. "Operating Manual Research Camera Models: STL-1001E, STL-1301E, STL-4020M, STL-6303E and STL-11000M." *SBIG Astronomical Instruments*. https://www.sbig.com/site/assets/files/18228/stl_operating_manual.pdf.

———. 2003b. "Users Guide: CCDOps Version 5." http://www.physics.csbsju.edu/ccd/manuals/CCDops_v5.pdf.

Starizona. 2014. "Calibration Images." *Starizona: Adventures in Astronomy and Nature*. https://starizona.com/acb/ccd/advimcal.aspx.

Swinburne. 2016. "Interstellar Reddening." *Cosmos*. http://astronomy.swin.edu.au/cosmos/I/Interstellar+Reddening.